A *N*-Phosphinoamidinato NHC-Diborene Catalyst for Hydroboration

Jun Fan,[a] Jian-Qiang Mah,[a] Ming-Chung Yang,[b] Ming-Der Su,*[b,c] and Cheuk-Wai So*[a]

[a]Division of Chemistry and Biological Chemistry, School of Physical and Mathematical Sciences, Nanyang Technological University, Singapore 637371. [b]Department of Applied Chemistry, National Chiayi University, Chiayi 60004, Taiwan. [c]Department of Medicinal and Applied Chemistry, Kaohsiung Medical University, Kaohsiung 80708, Taiwan.

ABSTRACT: The use of a *N*-phosphinoamidinato NHC-diborene catalyst **2** for hydroboration is described. The *N*-phosphinoamidine $tBu_2PN(H)C(Ph)=N(2,6\text{-}iPr_2C_6H_3)$ was reacted with *n*BuLi in Et_2O to afford the lithium derivative, which was then treated with $B_2Br_4(SMe_2)_2$ in toluene to form the *N*-phosphinoamidinate-bridged diborane **1**. It was then reacted with N-heterocyclic carbene, IMe ($:C\{N(CH_3)C(CH_3)\}_2$), and excess potassium graphite at room temperature in toluene to give the *N*-phosphinoamidinato NHC-diborene compound **2**. It can stoichiometrically activate ammonia-borane and carbon dioxide. It also showed catalytic capability. 2 mol% of **2** catalyzed hydroboration of carbon dioxide (CO_2) with pinacolborane (HBpin) in deuterated benzene (C_6D_6) at 110 °C (Conversion: >99%), which afforded methoxyborane [pinBOMe] (Yield: 97.8%, TOF: 33.3 h^{-1}) and bis(boryl)oxide [$(pinB)_2O$]. In addition, 5 mol% of **2** catalyzed N-formylation of secondary and primary amines by carbon dioxide and pinacolborane to yield the N-formamides (Average yield: 91.6%, TOF: 25.9 h^{-1}). Moreover, **2** showed chemoselectivity toward catalytic hydroboration of carbonyl compounds. In mechanistic studies, the B=B double-bond in compound **2** activated the substrates, the intermediates of which then underwent hydroboration with pinacolborane to yield the products and regenerate catalyst **2**.

Introduction

Multiply bonded main-group compounds containing a E=E double-bond (E = main-group element) or E≡E triple-bond are of particular interest as they exhibit transition-metal-like reactivity to activate and functionalize small molecules due to possession of HOMO and LUMO with small energy difference.[1] As an illustration, stable diboryne, diborene, dialumene, disilene, digermyne and distannyne were capable of non-catalytically activating a diversity of small molecules, namely dihydrogen, ammonia, nitrous oxide, carbon monoxide and carbon dioxide.[2-4] However, reversible activation is scarcely found, whereby only the distannyne [$Ar^{iPr}SnSnAr^{iPr}$] (Ar^{iPr} = C_6H_3-2,6-Ar_2, Ar = 2,6-$iPr_2C_6H_3$) reversibly underwent cycloaddition with ethylene and norbornadiene,[5] in addition to the reversible oxidation with H_2.[6] These results indicate that small molecules are difficult to dissociate from the main-group element centers after activation. As such, catalytic organic transformations mediated by multiply bonded main-group compounds are rare, with only two examples reported. The first example was digermyne-catalyzed cyclotrimerization of terminal alkynes, where the digermyne [TbbGeGeTbb] (Tbb = 4-*t*Bu-2,6-$[CH(TMS)_2]$-C_6H_2, TMS = $SiMe_3$) was a pre-catalyst (Figure 1), which reacted with alkyne to afford the digermabenzene.[7] It acted as the active catalyst to react with three more molecules of alkynes to form 1,2,4-triarylbenzene with high regioselectivity. The second example was the dialumene-catalyzed CO_2 hydroboration, where the NHC-dialumene [(IPrMe)(tBu_2MeSi)AlAl(SiMetBu_2)(IPrMe)] (IPrMe = $:C\{N(iPr)_2C(Me)\}_2$) was a pre-catalyst, which reacted with CO_2 to form a Al(μ-CO_3)(μ-O)Al six-membered ring.[8] It acted as the active catalyst to react with HBpin and CO_2 to form formoxyborane. In these catalyses, the Al=Al and Ge≡Ge multiple bonds were not able to regenerate after the catalytic cycle. These results give rise to the question of whether main-group multiple bond can involve in a catalytic cycle.

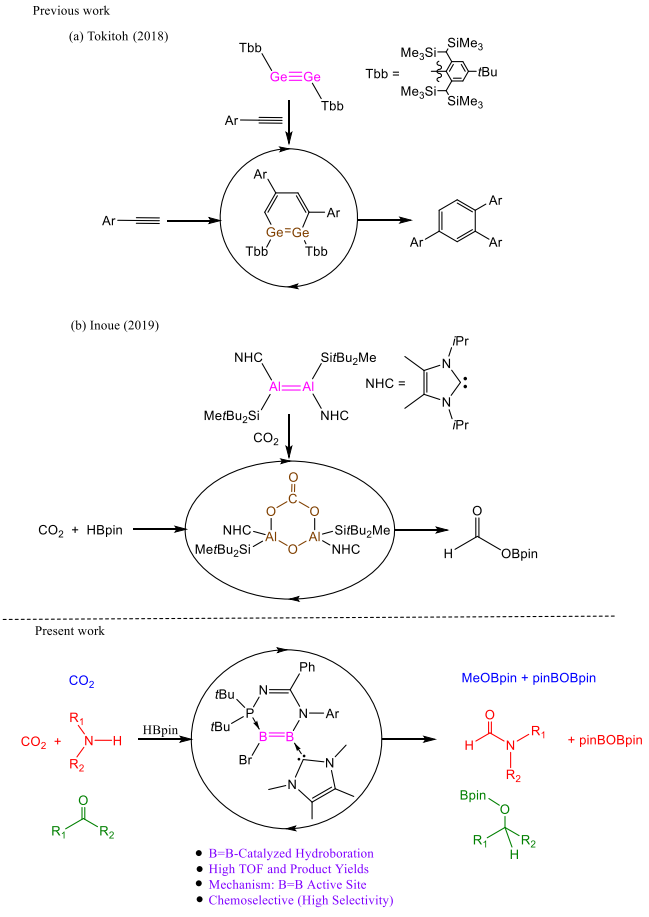

Figure 1. Multiply bonded main-group compounds for catalytic organic reactions.

To proof the concept, we were interested in synthesizing a main-group element multiply bonded delocalized compound for catalytic organic reactions because the delocalization effect could facilitate restoration of the main-group element multiple bond after a catalytic cycle. In this article, we report the synthesis of a *N*-phosphinoamidinato N-heterocyclic carbene-diborene catalyst and its application toward catalytic hydroboration of CO_2, catalytic N-formylation reaction of secondary and primary amines by carbon dioxide and pinacolborane, as well as chemoselective catalytic hydroboration of carbonyl compounds. DFT calculations are also reported to rationalize our experimental findings.

Results and Discussion

To begin with, the *N*-phosphinoamidine[9] was reacted with *n*BuLi in Et_2O for 3 h to afford the lithium derivative, which was then reacted with $B_2Br_4(SMe_2)_2$[10] in toluene for 12 h (Scheme 1). The LiBr formed in the reaction mixture was separated by filtration. After that, the filtrate was concentrated to afford the *N*-phosphinoamidinate-bridged diborane **1** as colorless crystals. The $^{11}B\{^1H\}$ NMR spectroscopy shows two signals at 55.5 and -11.9 ppm for sp^2 and sp^3 boron centers, respectively. The $^{31}P\{^1H\}$ NMR spectroscopy shows one signal at 35.9 ppm. X-ray crystallography of **1** shows that the ligand is bridged between two boron centers, where the length of B1-B2 bond is 1.704(5) Å (Figure 2). Moreover, the length of N1-B1 bond is 1.428(5) Å, indicating that the N1 lone pair of electrons delocalize to the vacant p orbital of the B1 center more than the amidinate N1-C13-N2 skeleton (C13-N2: 1.279(4) Å, C13-N1: 1.423(4) Å).

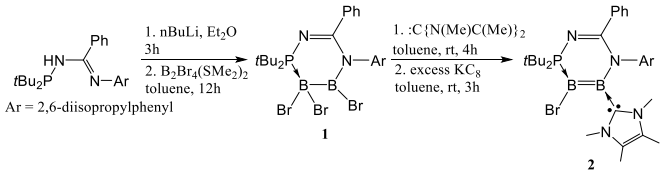

Scheme 1. Synthesis of **2**.

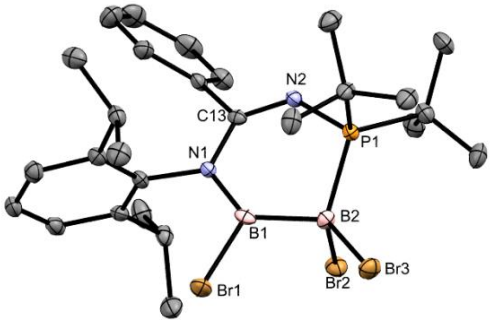

Figure 2. Molecular structure of **1** obtained by X-ray crystallography. Thermal ellipsoids are set at 50 % probability. All hydrogen atoms are deleted for clarity. Selected bond lengths (Å) and angles (deg): B1-B2 1.704(5), P1-B2 1.940(4), N1-B1 1.428(5), N1-C13 1.423(4), N2-C13 1.279(4), P1-N2 1.673(3), N1-B1-B2 124.3(3), B1-B2-P1 103.9(2), B2-P1-N2 104.53(15), P1-N2-C13 127.8(2), N2-C13-N1 126.3(3), C13-N1-B1 120.8(3).

Compound **1** was reacted with IMe ($:C\{N(CH_3)C(CH_3)\}_2$) at room temperature in toluene for 4 h to yield a red precipitate, which was then reacted with excess KC_8 in toluene for 3 h at room temperature to yield a purple-red mixture (Scheme 1). The precipitate (graphite and KBr) formed in the reaction mixture was removed by filtration. After that, the filtrate was concentrated to afford the phosphinoamidinato NHC-diborene compound **2** as a red crystalline solid. The $^{11}B\{^1H\}$ NMR spectroscopy displays 2 signals at 28.8 and 10.5 ppm, indicating that compound **2** is composed of a highly polarized B=B double-bond. The signals are in the range of the ^{11}B NMR signals (12 – 32 ppm) of similar Lewis base-diborene complexes.[11-25] The $^{31}P\{^1H\}$ NMR signal (45.9 ppm) is downfield shifted when comparing with that of **1**. The $^{13}C\{^1H\}$ NMR signal at 152.9 ppm is attributable to the $C_{carbene}$ center coordinating with the boron atom. The molecular structure of compound **2** obtained by X-ray crystallography is composed of a planar boron-containing six-membered ring with the N2-C1-N1-B2 torsion angle of -0.07° (Figure 3). This indicates that there is 6π-electron delocalization along the N2-C1-N1-B1-B2 skeleton. The N1 lone pair electrons delocalize along the amidinate skeleton, as indicated by the length of C1-N1 and C1-N2 bonds. This results in lengthening of N-B bond length (N1-B1: 1.526(4) Å) in comparison with that of **1**. The length of B2-B1 bond (1.562(5) Å) falls in the range of B=B double-bond length (1.546–1.625 Å) in similar Lewis base-diborene complexes.[11-25] The NHC (B1-C20: 1.590 Å) and phosphine (P1-B2: 1.852(3) Å) of the phosphinoamidinate ligand are bonded with the B=B bond. Their bond lengths are similar to those of other NHC/Phosphine-diborene complexes (C-B: 1.532 – 1.603 Å; P-B: 1.863 – 1.929 Å).[11-25]

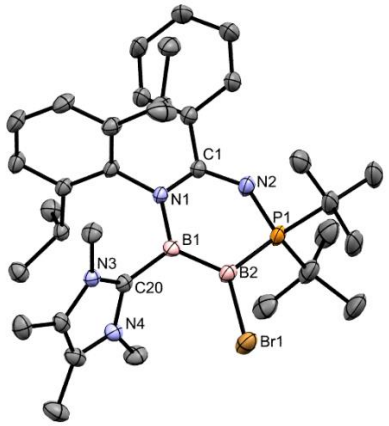

Figure 3. Molecular structure of **2** obtained by X-ray crystallography. Thermal ellipsoids are shown at 50 % probability. All hydrogen atoms are removed for clarity. Selected bond lengths (Å) and angles (deg): B2-B1 1.562(4), P1-B2 1.851(4), N1-B1 1.526(4), N2-P1 1.641(2), C1-N2 1.312(4), N1-C1 1.366(4); N1-B1-B2 123.8(3), B1-B2-P1 112.5(2), B2-P1-N2 106.45(14), P1-N2-C1 129.8(2), N2-C1-N1 125.0(3).

DFT calculations (M06-2X/def2-TZVP, Fig. S68) were performed to elucidate the electronic structure of **2**. The HOMO−1 shows the σ orbital of the B=B double-bond arising from the mixing of B 2p orbitals (Figure 4). The HOMO exhibits the π orbital of the B=B double-bond, while the LUMO represents the N 2p orbital conjugated with the π system of the phenyl group. Accordingly, the natural bond orbital (NBO, Table S8) analysis illustrates that the B1-B2 σ bond is arisen from the mixing of sp hybrids on the boron atoms (B1: $sp^{1.31}$; B2: $sp^{1.41}$). The B1-B2 π bond is slightly polarized toward the B1 atom (54.2 % B1 + 45.8 % B2). It is generated by the mixing of B p orbitals. The Wiberg Bond Index of 1.55 suggests

that the B2-B1 is a double bond. In addition, Natural Population Analysis (NPA) shows that the charge on the B1 and B2 atoms are −0.55 and 0.09 e, respectively. The dissected nucleus independent chemical shift ($NICS_{zz}$(1): -4.6 ppm, Table S9) shows that the diboron-containing six-membered ring in **2** is slightly aromatic.

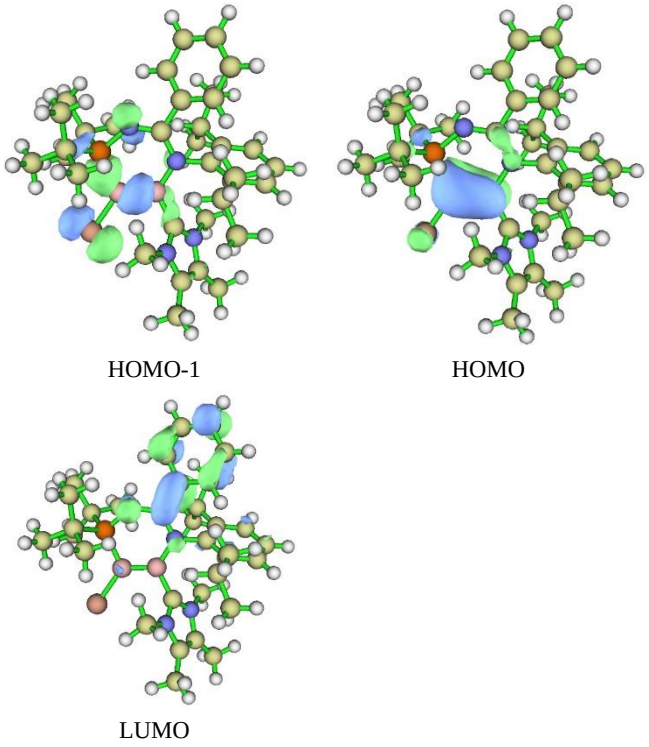

Figure 4. Calculated frontier orbitals of compound **2** (B: pink, Br: brown, C: yellow, H: white, N: blue, P: orange).

The B=B double-bond character in **2** was illustrated by its reactivity with NH_3BH_3 in toluene at -78 ºC (Scheme 2). The reaction mixture was warmed to room temperature and stirred for 3 h. The precipitate formed was discarded by filtration. After that, the borylboronium cation **3** was isolated as a colorless crystalline solid from the concentrated filtrate. It is proposed that the reaction proceeds through the addition of H^+ and H^- from NH_3BH_3 to the B=B double-bond in **2** to form a diborane intermediate **I** and NH_2BH_2. The second pair of H^+ and H^- from NH_2BH_2 attacks the *N*-phosphinoamidinate ligand and NHC-borane center, respectively, to form the *N*-phosphinoamidine ligand, which then displaces the Br^- moiety to form **3**. Its ^{1}H NMR spectrum exhibits signals for the *N*-phosphinoamidine and IMe backbone. The B–*H* signal cannot be found in the spectrum due to quadrupolar boron nucleus. The $^{31}P\{^1H\}$ NMR spectrum shows a multiplet at 85.6 ppm due to the coupling with N-H and B-H protons. The $^{11}B\{^1H\}$ NMR spectrum shows two broad signals for the boronium cation (-14.2 ppm) and borane center (-36.2 ppm). The molecular structure of **3** obtained by X-ray crystallography (Figure 5) illustrates that the *N*-phosphinoamidine chelates to the boronium B1 cation, while IMe coordinates to the borane B2 atom (C28-B2: 1.603(3) Å). Both boron centers adopt a tetrahedral geometry. The B1···Br distance is 9.331 Å, indicating that there is no interaction between these atoms. The length of B2-B1 bond is 1.749(4) Å. It is comparable to the B-B single bond length in compound **1** (1.704(5) Å). The N1-B1 bond (1.617(3) Å) is considerably lengthened when compared with the N-B single bond length (1.428(5) Å) in compound **1** indicating that the former is a coordinative covalent bond. In addition, the B1-P1 bond (1.970(2) Å) is comparable with the B-P coordinative covalent bond (1.940(4) Å) in compound **1**. These data support that the *N*-phosphinoamidine ligand chelates the boronium B1 cation.

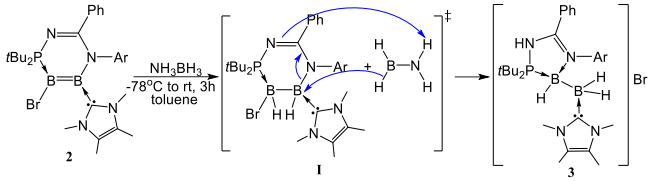

Scheme 2. Synthesis of **3.**

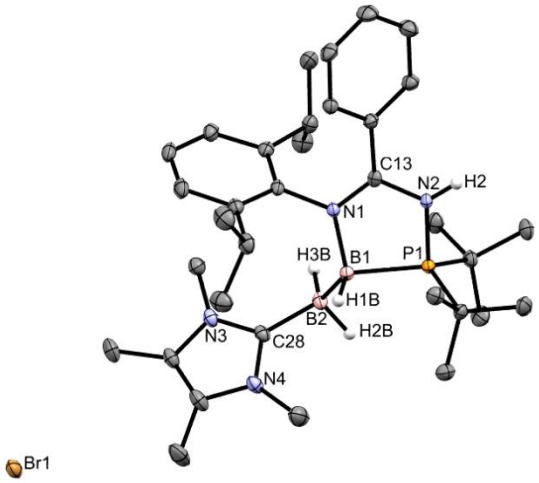

Figure 5. Molecular structure of **3** obtained by X-ray crystallography. Thermal ellipsoids are displayed at 50 % probability. All H atoms are omitted for clarity. Selected bond lengths (Å) and angles (deg): B2-B1 1.749(4), C28-B2 1.603(3), N1-B1 1.617(3), P1-B1 1.970(2), P1-N2 1.6987(19), N2-C13 1.360(3), N1-C13 1.313(3), N1-B1-P1 96.19(14), N1-B1-B2 120.62(19), P1-B1-B2 116.79(16), B1-B2-C28 114.2(2).

Compound **2** was capable of activating small molecule, namely carbon dioxide (CO_2, 1 atm) in toluene at room temperature (Scheme 3). The reaction mixture changed from reddish purple to colorless immediately. After filtering the reaction mixture, compound **4** was isolated as a colorless crystalline solid from the concentrated filtrate. In the reaction, the B=B double-bond in **2** undergoes a [2+2] cycloaddition with CO_2 to give compound **4**. Its spectrum of ^{1}H NMR spectroscopy displays signals of the *N*-phosphinoamidinate and IMe ligand. The $^{11}B\{^1H\}$ NMR signals are -5.5 and -17.9 ppm, which are upfield shifted comparing with that of compound **2**, demonstrating that the boron centers are four-coordinate. Moreover, the $^{31}P\{^1H\}$ NMR signal (39.7 ppm), which is comparable with that of compound **1**, is upfield shifted when compared with that of compound **2**. These spectroscopic data indicate that the B-B bond in compound **4** is a single bond. It is consistent with the molecular structure of **4** (Figure 6) obtained by X-ray crystallography where the length of B-B bond (1.770(3) Å) is comparable with the length of B-B single bond in compound **1**. The B_2CO four-membered ring is planar with the endocyclic O1-C28 bond (1.349(3) Å) being longer than

the exocyclic O2-C28 bond (1.218(3) Å). In addition, the Br and IMe moieties are positioned in a *cis* fashion in reference to the boron-containing four-membered ring. Compound **4** is stable in solution and the solid state, which does not decompose in refluxing toluene. Recently, Braunschweig et al. reported that the treatment of the NHC-diborene [IPr(Br)BB(Br)IPr] (IPr = :C{N(2,6-*i*Pr$_2$C$_6$H$_3$)CH}$_2$) with CO_2 formed a [2+2] cycloaddition product, which was thermally unstable and could not be isolated in quantity. It rearranged to form the 2,4-diboraoxetan-3-one containing oxo and carbonyl groups bridged between two boron centers.[26]

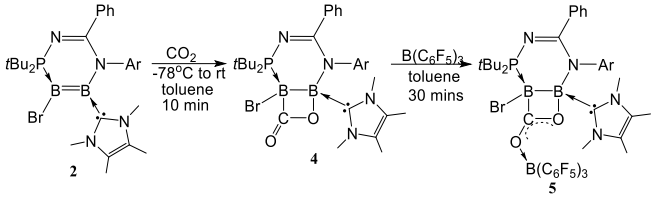

Scheme 3. Formation of compound **4** and **5.**

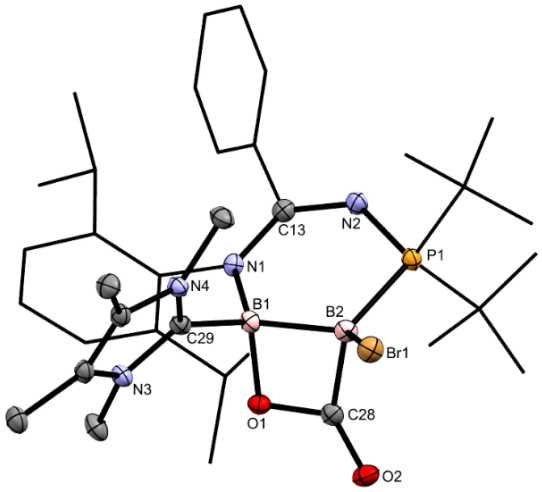

Figure 6. Molecular structure of **4** obtained by X-ray crystallography. Thermal ellipsoids are illustrated at 50 % probability. All hydrogen atoms are erased for clarity. Selected bond lengths (Å) and angles (deg): B2-B1 1.770(3), B2-C28 1.625(3), B1-O1 1.538(3), O1-C28 1.349(3), O2-C28 1.218(3), B2-P1 1.940(2), B1-N1 1.562(3), B1-C29 1.632(3), N1-B1-B2 118.67(17), B1-B2-P1 109.43(14), B1-B2-C28 78.73(15), B2-C28-O1 98.72(17), C28-O1-B1 96.48(15), O1-B1-B2 86.06(15).

It is anticipated that the activated CO_2 moiety in compound **4** can further be functionalized. As such, compound **2** was treated with CO_2 and tris(pentafluorophenyl)borane in toluene at room temperature, where the reaction color instantly changed from red-purple to colorless (Scheme 3). After stirring for 30 min, the solution was filtered. Compound **5** was isolated as colorless crystals from the concentrated filtrate. The reaction proceeds through the formation of compound **4**, where the exocyclic C=O double-bond further coordinates to $B(C_6F_5)_3$ to form compound **5**. Its $^{11}B\{^1H\}$ NMR signals (-5.7, -20.3 ppm) are comparable with that of **4**, indicating the presence of a B_2CO four-membered ring. Moreover, the $^{11}B\{^1H\}$ NMR signal of -26.9 ppm is attributable to the four-coordinate $B(C_6F_5)_3$. The molecular structure of **5** obtained by X-ray crystallography illustrates that the electronic structure of the B_2CO four-membered ring in **5** is different from that of **4** (Figure 7). The O1-C28 (1.292(4) Å) and O2-C28 (1.280(4) Å) bond lengths are almost identical, indicating that the double-bond in exocyclic C=O bond delocalizes along the O_{endo}-C-O_{exo} skeleton. The B2-C28 (1.593(5) Å) is shortened and the B1-O1 (1.625(5) Å) bond is lengthened in comparison with those in compound **4**. The experimental results show that **5** should comprise of canonical forms as illustrated in Scheme 4.

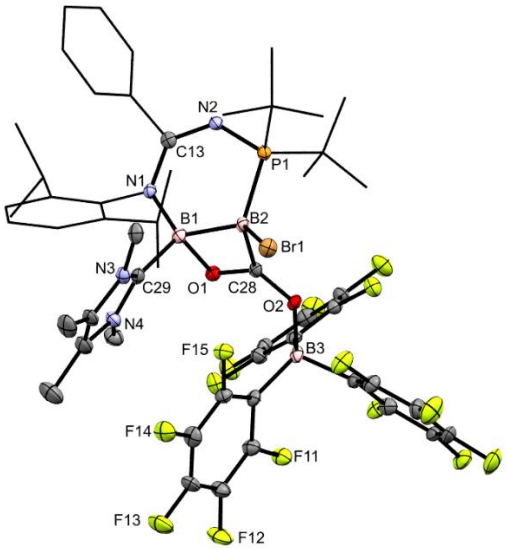

Figure 7. Molecular structure of **5** obtained by X-ray crystallography. Thermal ellipsoids are set at 50 % probability. All hydrogen atoms are deleted for clarity. Selected bond lengths (Å) and angles (deg): B1-B2 1.791(6), B2-C28 1.593(5), B1-O1 1.625(5), O1-C28 1.292(4), O2-C28 1.280(4), O2-B3 1.551(5), B2-P1 1.950(4), B1-N1 1.544(5), C29-B1 1.619(6), N1-B1-B2 121.2(3), O1-B1-B2 83.8(2), B1-B2-P1 106.6(2), B1-B2-C28 77.6(2), B2-C28-O1 104.2(3), C28-O1-B1 92.9(3), O1-C28-O2 122.7(3), B2-C28-O2 132.5(3), C28-O2-B3 128.1(3).

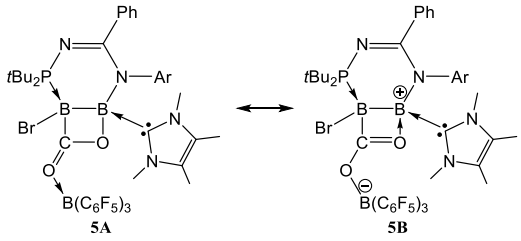

Scheme 4. Resonance structure of **5**

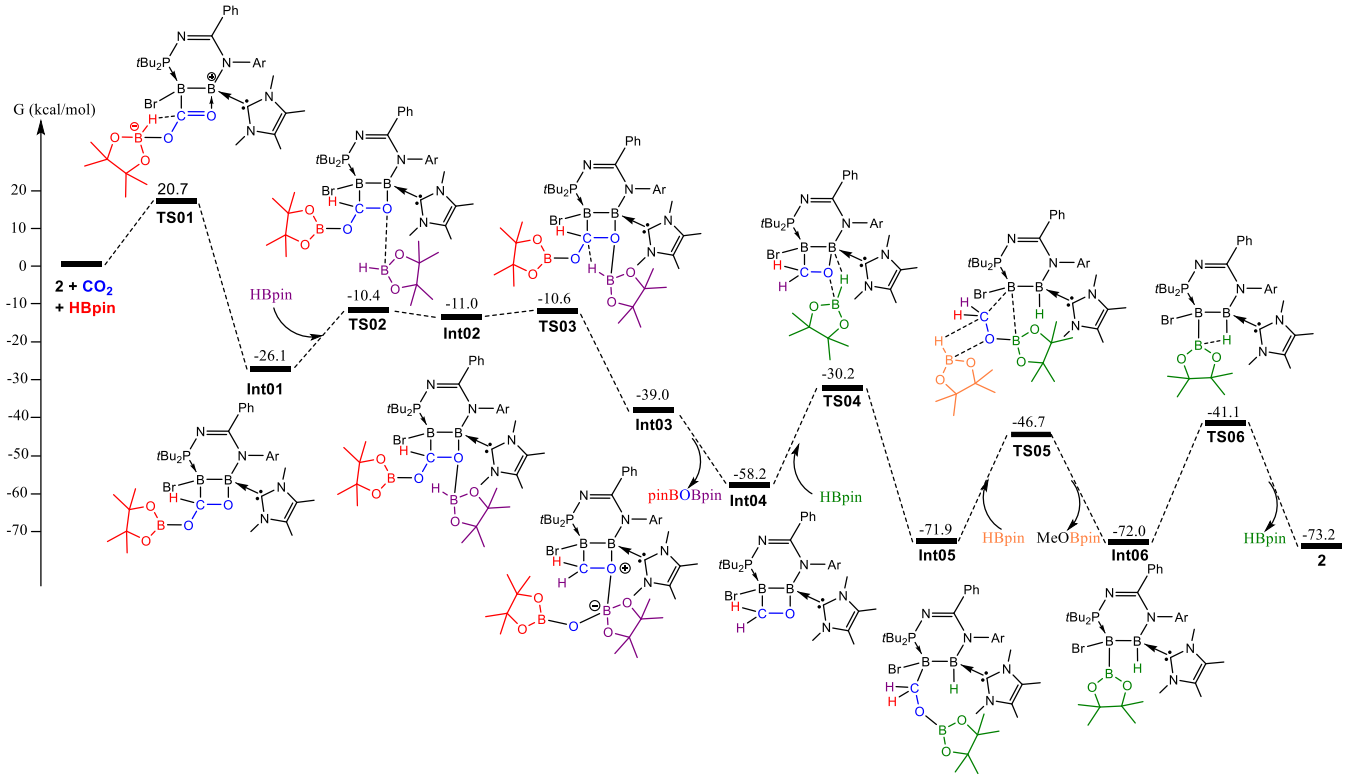

Scheme 6. DFT calculations of catalytic mechanism

It is anticipated that if $B(C_6F_5)_3$ in **5** is replaced by HBpin, the B-H bond could attack the C=O bond to form formoxyborane [pinBOC(O)H] and regenerate compound **2**. As such, compound **2** should show catalytic reactivity toward CO_2. To begin with, no reaction between carbon dioxide and pinacolborane in deuterated benzene (C_6D_6) at 110 °C was observed. 2 mol% of **2** was then used to catalyze reaction of CO_2 with HBpin in C_6D_6 at room temperature (Table S1). In the first 1 h, a mixture of formoxyborane [pinBOC(O)H] (**6a**, reaction time: 1 h, yield: 7.5%, Fig. S21) and bis(boryl)oxide [$(pinB)_2O$] (**6c**, reaction time: 1 h, yield: 8.2%) were formed. After 20 h, the conversion was still less than 30% and only **6c** was observed (reaction time: 20 h, yield: 26%). When reaction temperature increased to 110 °C (Scheme 5), the catalytic reaction was much more efficient and extremely clean (Conversion: >99%), forming a mixture of methoxyborane [pinBOMe] (**6b**, yield: 97.8%, TOF: 33.3 h^{-1}, Fig. S22) and **6c** in a 1:1 ratio. The activity of compound **2** is outstanding by considering turnover frequency and product yield. The turnover frequency (TOF) far surpasses those of main-group element hydride compounds (TOF, Mg: 0.07, Ca: 0.1, Ge: 2.1, Sn: 14.5 h^{-1}) for such catalysis.[27] Our results are different from the NHC-dialumene-catalyzed hydroboration of CO_2 with HBpin, where 80% conversion of CO_2 to [pinBOC(O)H] was achieved at 80 °C for 3 h via the dialuminum carbonate active catalyst.[8]

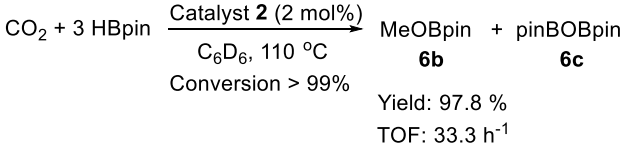

Scheme 5. Catalytic hydroboration of CO_2

When more sterically hindered 9-BBN (9-borabicyclo[3.3.1]nonane) was used instead of HBpin (Table S2, Fig. S25), 2 mol% of **2** catalyzed the hydroboration of CO_2 in C_6D_6 at 110 °C to form small amounts of formoxyborane **7a** at time zero. When the reaction continued to proceed, bis(boryl)acetal (**7b**, reaction time: 1 h, yield: 27.5%) and methoxyborane (**7c**, reaction time: 20 h, yield: 92%) were sequentially observed. The chronological formation of hydroborated products suggest that the B=B double-bond was recurrently restored in a catalytic cycle. Therefore, the B=B double-bond in compound **2** is the active site in the catalytic hydroboration of CO_2.

To prove that compound **4** is an intermediate in the catalysis, 2 mol% of **4** was utilized to mediate the catalytic reaction of carbon dioxide and pinacolborane in deuterated benzene (C_6D_6) at 110 °C for 2 h to afford a mixture of **6b** (Yield: 92.7%, TOF: 23.6 h^{-1}) and **6c** in a 1:1 ratio. This illustrates that compound **4** further reacts with HBpin to form a zwitterionic moiety in resemblance of compound **5**.

On the basis of these experimental studies, the catalytic cycle for the hydroboration of CO_2 with HBpin is proposed (Scheme 6) and studied by DFT calculations (M06-2X/def2-TZVP//M06-2X/def2-SVP/SMD(Benzene)). The B=B double-bond in **2** activates CO_2 with HBpin via **TS01** (ΔG = 20.7 kcal/mol). Subsequently, the H-B bond undergoes nucleophilic attack to the C=O bond to form **Int01** (ΔG = -26.1 kcal/mol). It appears as a [2+2] cycloaddition between **2** and a formoxyborane [HC(O)OBpin]. The second HBpin then coordinates with the acetal oxygen atom in **Int01** via **TS02** (ΔG = -10.4 kcal/mol) to give **Int02** (ΔG = -11.0 kcal/mol). Its B-H bond attacks the acetal carbon atom via **TS03** (ΔG = -10.6 kcal/mol), which induces nucleophilic attack of OBpin, lead-

ing to the formation of pinBOBpin coordinated to the formaldehyde oxygen atom in **Int03** (ΔG = -39.0 kcal/mol). At this point, it is obvious that the first two C-H bond formations are kinetically facile processes. The steric effect between IMe and pinBOBpin leads to dissociation of the latter to form **Int04** (ΔG = -58.2 kcal/mol). **Int04** is considered as a [2+2] cycloaddition product between **2** and a formaldehyde. The B-O bond in **Int04** then undergoes σ-bond metathesis reaction with the B-H bond of the third HBpin via **TS04** (ΔG = -30.2 kcal/mol) to form **Int05** (ΔG = -71.9 kcal/mol). The fourth HBpin coordinates with the O atom in **Int05**. The B-H bond subsequently attacks the methylene carbon via **TS05** (ΔG = -46.7 kcal/mol), which results in cleaving the B-$C_{methylene}$ bond and forming the B-Bpin bond, affording **Int06** and MeOBpin (ΔG = -72.0 kcal/mol). **Int06** undergoes 1,2-elimination of HBpin via **TS06** (ΔG = -41.1 kcal/mol) to generate **2** and HBpin (ΔG = -73.2 kcal/mol). The computed barriers of **Int04**→**TS04** (28.0 kcal/mol) and **Int06**→**TS06** (30.9 kcal/mol) are consistent with the catalysis requiring 110 °C to occur. The calculation results are in accordance with the experimental conditions and observations. Reaction temperature of 25 °C resulted in **6c** with 26% yield (20 h), suggesting that the reaction ends at **Int04**. Reaction temperature of 110 °C provides sufficient energy to overcome the kinetic barrier (**TS04** and **TS06**) and hence a mixture of **6b** and **6c** was formed in a 1:1 ratio.

Then, the catalytic ability of **2** towards N-formylation of primary and secondary amines, carbon dioxide and pinacolborane was examined (Table 1, Table S3). To begin with, compound **2** (5 mol%) cannot catalyze the reaction of **8e** and carbon dioxide at 90 °C without HBpin (Table S4). However, 5 mol% of **2** catalyzed the N-formylation of primary aliphatic n-butylamine **8b** and 3-methoxypropan-1-amine **8c**, with CO_2 and pinacolborane in deuterated benzene (C_6D_6) at 90 °C to yield the corresponding N-formamides [yield (TOF), **9b**: 95 (40.0), **9c**: 96% (40.0 h^{-1})], bis(boryl)oxide **6c** and H_2. Second, high yield and TOF were accomplished for the N-formylation of aliphatic secondary diethylamine **8d** (yield: 92%, TOF: 50 h^{-1}), diisopropylamine **8a** (yield: 98%, TOF: 13.3 h^{-1}) and piperidine **8e** (yield: 98%, TOF: 33.3 h^{-1}). Third, aromatic *N*-methylaniline **8f** (yield: 81%, TOF: 3.1 h^{-1}) and indoline (**8g**, yield: 91%, TOF: 1.4 h^{-1}) were less active in the catalyses. It is noteworthy that compound **2** is one of the rare main-group catalysts that mediate N-formylation using carbon dioxide and pinacolborane, including the NHC-silyliumylidene cation $[(IMe)_2SiH]I$.[28] Moreover, **2** exceeds the latter in view of both reaction time and TOF (Example of $[(IMe)_2SiH]I$, **9a**: Yield: 68%, TOF: 6.8 h^{-1}). Other main-group element catalysts, namely proazaphosphatrane[29] and carbodicarbene[30] can only use potent 9-BBN for the N-methylation of amines with carbon dioxide. To understand catalytic mechanism, piperidine **8e** was reacted with HBpin in C_6D_6 at 90 °C, resulting in the formation of the borylamine and H_2. This suggests that the formation of H_2 in the above catalysis arose from the coupling reaction of amines and HBpin. In this context, the catalytic mechanism is proposed (Scheme 7). Compound **2** catalyzes the reaction of CO_2 and HBpin to form formoxyborane [pinBOC(O)H] (**6a**). It then undergoes substitution reaction with borylamine, which is formed by the dehydrogenation reaction of amine and HBpin, to form N-formamide and pinBOBpin **6c**.

Table 1. **2**-catalyzed N-formylation[a]

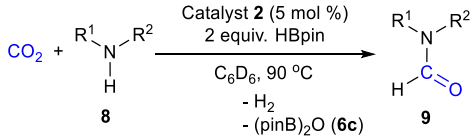

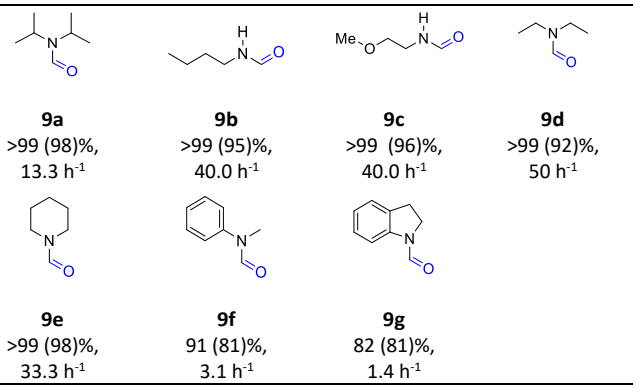

9a	**9b**	**9c**	**9d**
>99 (98)%, 13.3 h^{-1}	>99 (95)%, 40.0 h^{-1}	>99 (96)%, 40.0 h^{-1}	>99 (92)%, 50 h^{-1}

9e	**9f**	**9g**
>99 (98)%, 33.3 h^{-1}	91 (81)%, 3.1 h^{-1}	82 (81)%, 1.4 h^{-1}

[a]Reaction conditions: Amine (0.10 mmol), HBpin (0.20 mmol, 2 equiv.), **2** (5 mol%), C_6D_6 (0.50 mL), CO_2. Yields were calculated by ^1H NMR spectroscopy based on the amount of the consumed amine with reference to cyclohexane (internal standard). They were reported in parenthesis. $R^1R^2NC(O)H$ was identified as the sole product. All substrates were performed thrice.

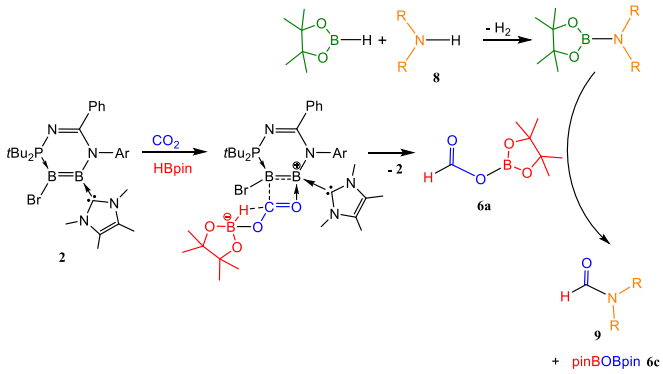

Scheme 7. Proposed catalytic N-formylation mechanism.

Besides catalytic hydroboration of carbon dioxide and N-formylation, **2** (5 mol%) was able to catalyze chemoselective hydroboration of aldehyde and ketone compounds **10** in C_6D_6 at room temperature to form borate esters (**11**, 16 examples, aldehydes: yield = 99%, TOF = 4 - 120 h^{-1}; ketones: yield = 80 - 98%, TOF = 0.4 - 10 h^{-1}, Scheme 8, Table S5). The results further support that compound **2** is an active catalyst in >C=O hydroboration.

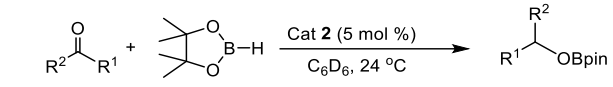

R^1 = H or Me
R^2 = alkyl or aryl substituents
10

Scheme 8. Chemoselective hydroboration of carbonyl compounds.

Conclusion

In conclusion, the phosphinoamidinato NHC-diborene compound **2** is a multiply bonded boron catalyst showing catalytic capability toward the hydroboration of CO_2 with HBpin, N-formylation of primary and secondary amines by CO_2 and HBpin, as well as chemoselective hydroboration of carbonyl compounds. In particular, compound **2** efficiently reduces CO_2 with HBpin to form MeOBpin and pinBOBpin. Its catalytic activity is superior to that of existing main-group element catalysts employed for such reaction. In the mechanistic studies, compound **2** exhibits reactivity resemble to transition metal in the catalytic hydroboration of CO_2. Its B=B double-bond activated CO_2 with HBpin, the initial intermediate of which was further reacted with HBpin molecules to form MeOBpin and pinBOBpin, along with the regeneration of **2**. It is anticipated that compound **2** can mediate a variety of other catalytic reactions and they are currently under investigation.

Experimental Section

General procedure. All experiments were performed under an argon gas atmosphere by standard Schlenk procedures. Chemicals were acquired from Sigma-Aldrich and utilized directly without further purification. All solvents were dried over K metal or CaH_2 prior to use. The ^{1}H, $^{11}B\{^{1}H\}$, $^{13}C\{^{1}H\}$ and $^{31}P\{^{1}H\}$ NMR spectroscopy were performed using a JEOL ECA 400 MHz spectrometer. All NMR spectra were recorded in deuterated benzene (C_6D_6). The chemical shifts (ppm) are respective to $SiMe_4$ for ^{13}C and ^{1}H; $BF_3{\cdot}Et_2O$ for ^{11}B; 85% H_3PO_4 for ^{31}P, respectively. HRMS spectrometry were performed at the Mass Spectrometry Laboratory in the Division of Chemistry and Biological Chemistry, Nanyang Technological University. Melting points were recorded using an OptiMelt automated melting point machine.

Synthesis of 1. A solution of *n*BuLi (2.6 M, 0.4 mL, 1.05 mmol) in hexane was added into a 100 mL Schlenk flask containing a stirring diethyl ether solution of *N*-phosphinoamidine (0.425 g, 1 mmol) at -78 °C, following which, the solution was warmed to room temperature and stirred for 3 h. The resulting yellow solution was dried under vacuum to remove all volatiles. A solution of $B_2Br_4(SMe_2)_2$ (0.466 g, 1 mmol) in toluene was then slowly added into the Schlenk flask at -78 °C. The reaction mixture was stirred at room temperature for 12 h. It was filtered. The filtrate was then concentrated and stood at 4 °C for two days to yield **1** as a colorless crystalline solid (0.52 g, 76% yield). M.p.: 177 °C. ^{1}H NMR (399.5 MHz, 25 °C, C_6D_6): δ 7.33-7.30 (m, 2 H, Ar*H*), 7.05-6.77 (m, 6 H, Ar*H*), 3.38 (sept, 2 H, C*H*Me$_2$, J_{HH} = 6.8 Hz), 1.44 (d, 18 H, *tBu*, J_{PH} = 14.2 Hz), 1.32 (d, 6 H, CH*Me$_2$*, J_{HH} = 6.8 Hz), 0.93 (d, 6 H, CH*Me$_2$*, J_{HH} = 6.8 Hz). $^{11}B\{^{1}H\}$ NMR (128 MHz, 25 °C, C_6D_6): δ 55.50 (s), -11.94 (s). $^{31}P\{^{1}H\}$ NMR (162 MHz, 25 °C, C_6D_6): δ 35.72 (br). $^{13}C\{^{1}H\}$ NMR (101 MHz, 25 °C, C_6D_6): 168.14 (d, J = 11.6 Hz, N*C*N), 145.41 (*C*H-Ar), 140.05 (*C*H-Ar), 138.74 (d, J = 13.5 Hz, *C*-Ar), 129.44 (*C*H-Ar), 128.89 (*C*H-Ar), 128.78 (*C*H-Ar), 128.45 (*C*H-Ar), 127.62 (*C*H-Ar), 126.99 (*C*-Ar), 124.45 (*C*-Ar), 38.28 (d, J = 34.8 Hz, P*C*(CH$_3$)), 28.62 (*C*H(CH$_3$)$_2$), 27.77 (PC(*C*H$_3$)), 25.14 (CH(*C*H$_3$)$_2$), 23.34 (CH(*C*H$_3$)$_2$). HRMS (ESI): *m/z* calcd for $C_{27}H_{41}B_2{}^{79}Br_3N_2P$: 683.0744 [(*M* + *H*)]$^+$; found: 683.0761.

Synthesis of 2. A toluene solution of 1,3,4,5-tetramethylimidazolin-2-ylidene (IMe, 0.149 g, 1.2 mmol) was added into a 100 mL Schlenk flask containing **1** (0.685 g, 1 mmol) at room temperature. After 10 minutes, the color of the reaction mixture turned red with some precipitate. The resulting suspension was stirred for 4 h. Subsequently, it was filtered and the pale red residue was then dried under vacuum for 2 h. The red residue was **1**·IMe adduct and used without further purification. 30 mL of toluene was added into a 100 mL Schlenk flask containing the mixture of **1**·IMe (0.809 g, 1 mmol) and excess potassium graphite (0.54 g, 4 mmol) at room temperature, turning the reaction mixture to purplish red immediately. The resulting suspension was stirred for 3 h and filtered. The filtrate was concentrated to 5 mL and stored at -20 °C for 1 day to get **2** as a red crystalline solid (0.24 g, 37% yield). M.p.: 198 °C (dec.). ^{1}H NMR (399.5 MHz, 25 °C, C_6D_6): δ 7.66-7.64 (m, 2 H, Ar*H*), 7.05-6.88 (m, 6 H, Ar*H*), 3.37 (sept, 2 H, C*H*Me$_2$, J_{HH} = 7.2 Hz), 3.19 (s, 6 H, N-C*H*$_3$), 1.71 (d, 18 H, *tBu*, J_{PH} = 12.8 Hz), 1.23 (s, 6 H, C-C*H*$_3$), 0.85 (d, 6 H, CH*Me$_2$*, J_{HH} = 6.4 Hz), 0.80 (d, 6 H, CH*Me$_2$*, J_{HH} = 6.8 Hz). $^{11}B\{^{1}H\}$ NMR (128 MHz, 25 °C, C_6D_6): δ 30.64, 9.16. $^{31}P\{^{1}H\}$ NMR (162 MHz, 25 °C, C_6D_6): δ 45.93 (br). $^{13}C\{^{1}H\}$ NMR (101 MHz, 25 °C, C_6D_6): 152.85 (*C*$_{\text{-carbene}}$), 145.37 (*C*H-Ar), 144.46 (*C*H-Ar), 141.05 (d, J = 16.4 Hz, *C*-Ar), 130.72 (*C*H-Ar), 129.01 (*C*H-Ar), 128.25 (*C*H-Ar), 127.62 (*C*H-Ar), 126.90 (*C*H-Ar), 126.70 (*C*-Ar), 126.65 (*C*-Ar), 124.13 (*C*-Ar), 123.04 (*C*CH$_3$), 38.65 (d, J = 42.5 Hz, P*C*(CH$_3$)), 33.13 (N*C*H$_3$), 28.47 (*C*H(CH$_3$)$_2$), 27.72 (d, J = 1.9 Hz, PC(*C*H$_3$)), 24.95 (CH(*C*H$_3$)$_2$), 23.55 (CH(*C*H$_3$)$_2$), 7.82 (*C*H$_3$). HRMS (ESI): *m/z* calcd for $C_{34}H_{53}B_2{}^{79}BrN_4P$: 649.3377 [(*M* + *H*)]$^+$; found: 649.3395.

Synthesis of 3. 20 mL of toluene was added into a 100 mL Schlenk flask containing **2** (0.130 g, 0.2 mmol) and NH_3BH_3 (0.007 g, 0.2 mmol) at -78 °C. The resulting solution was warmed to room temperature and stirred for 3 h with the color changing from red-purple to pale red. The reaction solution was filtered. The filtrate was then concentrated and kept at room temperature to give **3** as a colorless crystalline solid (0.07 g, 54% yield). M.p.: 147 °C. ^{1}H NMR (399.5 MHz, 25 °C, C_6D_6): δ 7.78-7.76 (m, 2 H, Ar*H*), 6.87-7.04 (m, 4 H, Ar*H*), 6.75-6.69 (m, 2 H, Ar*H*), 3.29 (sept, 1 H, C*H*Me$_2$, J_{HH} = 7.2 Hz), 2.78 (sept, 1 H, C*H*Me$_2$, J_{HH} = 7.2 Hz), 2.61 (s, 6 H, N-C*H*$_3$), 1.78 (dd, 18 H, *tBu*, J_{PH} = 14.2 Hz, J_{PH} = 15.1 Hz), 1.44 (d, 3 H, CH*Me$_2$*, J_{HH} = 6.4 Hz), 1.27 (s, 6 H, C-C*H*$_3$), 1.11 (d, 3 H, CH*Me$_2$*, J_{HH} = 6.8 Hz), 0.46 (d, 3 H, CH*Me$_2$*, J_{HH} = 6.8 Hz), 0.12 (d, 3 H, CH*Me$_2$*, J_{HH} = 6.8 Hz). $^{11}B\{^{1}H\}$ NMR (128 MHz, 25 °C, C_6D_6): δ -14.24 (br), -34.15 (br). $^{31}P\{^{1}H\}$ NMR (162 MHz, 25 °C, C_6D_6): δ 85.62 (br). $^{13}C\{^{1}H\}$ NMR (101 MHz, 25 °C, C_6D_6): 167.13 (d, J = 11.5 Hz, N*C*N), 145.90 (*C*$_{\text{-carbene}}$), 144.89 (*C*H-Ar), 143.81 (*C*H-Ar), 139.24 (d, J = 8.6 Hz, *C*-Ar), 132.17 (*C*H-Ar), 131.83 (*C*H-Ar), 130.23 (*C*H-Ar), 126.70 (*C*H-Ar), 126.11 (*C*H-Ar), 125.25 (*C*-Ar), 124.63 (*C*-Ar), 124.38 (*C*-Ar), 123.74 (*C*CH$_3$), 121.75 (*C*CH$_3$), 37.72 (d, J = 23.1 Hz, P*C*(CH$_3$)), 35.50 (d, J = 25.1 Hz, P*C*(CH$_3$)), 34.68 (N*C*H$_3$), 31.50 (N*C*H$_3$), 28.64 (*C*H(CH$_3$)$_2$), 28.08 (d, J = 28.9 Hz, PC(*C*H$_3$)), 27.74 (d, J = 28.9 Hz, PC(*C*H$_3$)), 25.48 (*C*H(CH$_3$)$_2$), 24.80 (CH(*C*H$_3$)$_2$), 23.94 (CH(*C*H$_3$)$_2$), 23.10 (CH(*C*H$_3$)$_2$), 22.67 (CH(*C*H$_3$)$_2$), 7.89 (*C*H$_3$), 7.58 (*C*H$_3$). HRMS (ESI): *m/z* calcd for $C_{34}H_{57}B_2{}^{79}BrN_4P$: 653.3690 [(*M* + *H*)]$^+$; found: 653.3705.

Synthesis of 4. A toluene solution of **2** (0.130 g, 0.2 mmol) in a Schlenk flask was degassed by a freeze–pump–thaw method. Then, CO_2 (1 bar) was filled. The resulting solution changed from reddish purple to colorless immediately. After 10 minutes of stirring, the solution was filtered. The filtrate was concentrated and kept at – 20 °C for one day to get **4** as a colorless crystalline solid (0.12 g, 88% yield). M.p.: 193 °C. ^{1}H NMR (399.5 MHz, 25 °C, C_6D_6): δ 7.66-7.64 (m, 2 H, Ar*H*), 7.14-7.02 (m, 2 H, Ar*H*), 6.92-6.88 (m, 3 H, Ar*H*),

6.79-6.75 (m, 1 H, Ar*H*), 3.83 (sept, 1 H, C*H*Me$_2$, J_{HH} = 7.2 Hz), 3.63 (s, 3 H, N-CH_3), 2.83 (sept, 1 H, C*H*Me$_2$, J_{HH} = 7.2 Hz), 2.61 (s, 3 H, N-CH_3), 1.69 (d, 3 H, CH*Me$_2$*, J_{HH} = 7.3 Hz), 1.67 (dd, 18 H, *tBu*, J_{PH} = 7.3 Hz, J_{PH} = 8.2 Hz), 1.37 (s, 3 H, C-CH_3), 0.92 (d, 3 H, CH*Me$_2$*, J_{HH} = 6.8 Hz), 0.87 (s, 3 H, C-CH_3), 0.74 (d, 3 H, CH*Me$_2$*, J_{HH} = 6.4 Hz), 0.09 (d, 3 H, CH*Me$_2$*, J_{HH} = 6.8 Hz). ^{11}B{^{1}H} NMR (128 MHz, 25 °C, C_6D_6): δ -5.47, -17.86. ^{31}P{^{1}H} NMR (162 MHz, 25 °C, C_6D_6): δ 39.66 (br). ^{13}C{^{1}H} NMR (101 MHz, 25 °C, C_6D_6): 168.72 (d, *J* = 8.7 Hz, N*C*N), 148.99 (*C*$_{\text{-carbene}}$), 144.31 (*C*H-Ar), 142.42 (*C*H-Ar), 141.10 (d, *J* = 15.4 Hz, *C*-Ar), 130.53 (*C*H-Ar), 128.52 (*C*H-Ar), 127.28 (*C*H-Ar), 127.10 (*C*H-Ar), 126.76 (*C*H-Ar), 125.71 (*C*-Ar), 124.72 (*C*-Ar), 124.45 (*C*-Ar), 123.88 (*C*CH$_3$), 123.72 (*C*CH$_3$), 38.46 (d, *J* = 44.3 Hz, P*C*(CH$_3$)), 38.08 (d, *J* = 44.3 Hz, P*C*(CH$_3$)), 34.37 (N*C*H$_3$), 31.85 (N*C*H$_3$), 28.64 (*C*H(CH$_3$)$_2$), 27.88 (d, *J* = 28.9 Hz, PC(*C*H$_3$)), 26.71 (*C*H(CH$_3$)$_2$), 25.66 (CH(*C*H$_3$)$_2$), 25.09 (CH(*C*H$_3$)$_2$), 24.86 (CH(*C*H$_3$)$_2$), 22.87 (CH(*C*H$_3$)$_2$), 7.53 (*C*H$_3$), 7.31 (*C*H$_3$). HRMS (ESI): *m/z* calcd for $C_{35}H_{53}B_2{}^{79}BrN_4O_2P$: 693.3276 [(*M* + *H*)]$^+$; found: 693.3302.

Synthesis of 5. A toluene solution of **2** (0.130 g, 0.2 mmol) and tri(pentafluorophenyl)borane (0.110 g, 0.2 mmol) in a Schlenk flask was degassed by a freeze–pump–thaw method. Subsequently, CO_2 (1 bar) was filled. The resulting solution changed from red-purple to colorless immediately. After 30 minutes of stirring, the solution was filtered. The filtrate was concentrated and kept at – 20 °C for one day to afford **5** as a colorless crystalline solid (0.20 g, 84% yield). M.p.: 161 °C. ^{1}H NMR (399.5 MHz, 25 °C, C_6D_6): δ 7.27-7.25 (m, 2 H, Ar*H*), 7.08-6.90 (m, 2 H, Ar*H*), 6.80-6.78 (m, 3 H, Ar*H*), 6.64-6.61 (m, 1 H, Ar*H*), 3.56 (s, 3 H, N-CH_3), 2.82 (sept, 1 H, C*H*Me$_2$, J_{HH} = 7.2 Hz), 2.49 (sept, 1 H, C*H*Me$_2$, J_{HH} = 7.2 Hz), 2.14 (s, 3 H, N-CH_3), 1.42 (dd, 18 H, *tBu*, J_{PH} = 13.7 Hz, J_{PH} = 15.1 Hz), 1.42 (s, 3 H, C-CH_3), 1.13 (s, 3 H, C-CH_3), 0.95 (d, 3 H, CH*Me$_2$*, J_{HH} = 6.4 Hz), 0.81 (d, 3 H, CH*Me$_2$*, J_{HH} = 6.8 Hz), 0.21 (d, 3 H, CH*Me$_2$*, J_{HH} = 6.8 Hz), 0.10 (d, 3 H, CH*Me$_2$*, J_{HH} = 6.8 Hz). ^{11}B{^{1}H} NMR (128 MHz, 25 °C, C_6D_6): δ -5.71, -20.32, -26.89. ^{19}F{^{1}H} NMR (376 MHz, 25 °C, C_6D_6): δ -131.31 (s, 1 F), -159.34 (t, 1 F, *J* = 21.7 Hz), -164.69 (dt, 1 F, *J* = 21.7, 21.7 Hz). ^{31}P{^{1}H} NMR (162 MHz, 25 °C, C_6D_6): δ 37.44 (br). ^{13}C{^{1}H} NMR (101 MHz, 25 °C, C_6D_6): δ 168.48 (d, *J* = 8.7 Hz, N*C*N), 149.56 (*C*-F), 147.42 (*C*$_{\text{-carbene}}$), 147.11 (*C*-F), 144.05 (*C*H-Ar), 141.74 (*C*H-Ar), 139.66 (d, *J* = 16.3 Hz, *C*-Ar), 138.33 (*C*-F), 137.58 (*C*-F), 135.73 (*C*-F), 130.89 (*C*H-Ar), 129.27 (*C*H-Ar), 129.01 (*C*H-Ar), 128.24 (*C*H-Ar), 127.61 (*C*H-Ar), 126.81 (*C*-Ar), 126.16 (*C*-Ar), 125.95 (*C*-Ar), 125.72 (*C*-Ar), 125.37 (*C*CH$_3$), 123.58 (*C*CH$_3$), 39.34 (d, *J* = 45.7 Hz, P*C*(CH$_3$)), 37.94 (d, *J* = 39.5 Hz, P*C*(CH$_3$)), 35.79 (N*C*H$_3$), 32.10 (N*C*H$_3$), 28.31 (d, *J* = 38.5 Hz, PC(*C*H$_3$)), 27.54 (*C*H(CH$_3$)$_2$), 26.82 (*C*H(CH$_3$)$_2$), 25.03 (CH(*C*H$_3$)$_2$), 24.21 (CH(*C*H$_3$)$_2$), 22.20 (CH(*C*H$_3$)$_2$), 21.11 (CH(*C*H$_3$)$_2$), 7.60 (*C*H$_3$), 7.53 (*C*H$_3$). HRMS (ESI): *m/z* calcd for $C_{53}H_{53}B_3{}^{79}BrF_{15}N_4O_2P$: 1205.3129 [(*M* + *H*)]$^+$; found: 1205.3145.

Synthesis of compound 6a – 6c. Catalyst **2** (0.026 g, 0.04 mmol), cyclohexane (internal standard, 0.168 g, 2 mmol, 50 equivalents) and deuterated benzene (C_6D_6, 0.5 ml) were added in a J-Young NMR tube. HBpin (0.256 g, 2 mmol, 50 equivalents) was subsequently added. After that, the J-Young NMR tube was dipped in liquid nitrogen and frozen the reaction mixture. It was degassed using freeze-pump-thaw cycle. Carbon dioxide (1 bar) was subsequently filled. The reaction mixture was warmed from room temperature to 110 °C for 1.5 hours. The catalysis was monitored using ^{1}H NMR spectroscopy. The yields were calculated based on the integration of ^{1}H NMR signals of pinBOMe (**6b**) at 1.05, 3.51 ppm and (pinB)$_2$O (**6c**) at 1.02 ppm relative to that of the –CH_2 of cyclohexane (internal standard) at 1.37 ppm. The chemical shifts of the products agree with the reported values in the literature and independent *in-situ* NMR-scale syntheses.[31]

Synthesis of compounds 7a – 7d. Catalyst **2** (1.3 mg, 0.002 mmol), 9-BBN (0.012g, 0.1 mmol, 50 equivalents) and C_6D_6 (0.5 mL) were added in a J-Young NMR tube. The solution was degassed by freeze–pump–thaw method as described in the synthesis of **6a** - **6c**. Carbon dioxide (1 bar) was then filled. After that, the resulting mixture was warmed from room temperature to 110 °C. The catalysis was checked by ^{1}H NMR spectroscopy at time intervals of 20 minutes, 40 minutes, 1 h, 4 h, 12 h and 20 h. The NMR data are written in the Supporting Information.

Catalytic N-formylation of primary and secondary amines by CO_2 and HBpin (General procedure). Catalyst **2** (0.0032 g, 0.005 mmol), cyclohexane (internal standard, 8.4 mg, 0.10 mmol), HBpin (0.0256 g, 0.20 mmol), amine (0.10 mmol) and deuterated benzene (C_6D_6, 0.5 mL) were added in a J-Young NMR tube. Subsequently, the latter was dipped in liquid nitrogen and the reaction mixture was frozen. It was degassed using freeze-pump-thaw cycle. Carbon dioxide (1 bar) was subsequently filled. The details of catalytic settings are stated in Table S3 – S4 in the Supporting Information. The catalysis was checked by ^{1}H NMR spectroscopy. The yields of products were calculated on the basis of the integration of ^{1}H NMR signals of R^{1}R^{2}NC(=O)*H* at *ca.*8 ppm relative to that of cyclohexane (CH_2, 1.37 ppm). The NMR data are written in the Supporting Information.

Catalytic reaction of aldehydes and ketones with HBpin (General procedures). Catalyst **2** (0.013 g, 0.02 mmol) and C_6D_6 (0.5 mL) were mixed in a J-Young NMR tube. Pinacolborane (0.052 g, 0.41 mmol, 20.1 equivalents) and carbonyl compounds (0.40 mmol, 20 equivalents) were subsequently mixed. The catalytic settings are stated in Table S5. The catalyses were checked by ^{1}H NMR spectroscopy to calculate their yields. The chemical shifts of the products are consistent with the reported values in the literatures.[31] All the catalytic trials were performed thrice.

ASSOCIATED CONTENT

Supporting Information. The Supporting Information is available free of charge on the ACS Publications website.

Experimental procedures and DFT calculations (PDF)
X-ray crystallographic data for compounds **1** - **5** (CIF).

AUTHOR INFORMATION

Corresponding Author

*CWSo@ntu.edu.sg
*midesu@mail.ncyu.edu.tw

Author Contributions

The manuscript was written through contributions of all authors.

ACKNOWLEDGMENT

C.-W.S. thanks the National Research Foundation Singapore, NRF-ANR (NRF2018-NRF-ANR026 Si-POP) and Ministry of Education Singapore, AcRF Tier 2 (MOE2019-T2-2-129) for the financial support. M.-C. Yang and M.-D. Su acknowledge the National Center for High-Performance Computing of Taiwan for generous amounts of computing time, and the Ministry of Science and Technology of Taiwan for the financial support.

REFERENCES

(1) (a) Power, P. P. Main-group Elements as Transition Metals. *Nature* **2010**, *463*, 171-177. (b) Braunschweig, H.; Dewhurst, R. D. Single, Double, Triple Bonds and Chains: The Formation of Electron-Precise B−B Bonds. *Angew. Chem., Int. Ed.* **2013**, *52*, 3574-3583. (c) Arrowsmith, M.; Braunschweig, H.; Stennett, T. E. Formation and Reactivity of Electron-Precise B−B Single and Multiple Bonds. *Angew. Chem., Int. Ed.* **2017**, *56*, 96-115. (d) Weetman, C.; Inoue, S. The Road Travelled: After Main-Group Elements as Transition Metals. *ChemCatChem* **2018**, *10*, 4213-4228. (e) Chu, T.; Nikonov, G. I. Oxidative Addition and Reductive Elimination at Main-Group Element Centers. *Chem. Rev.* **2018**, *118*, 3608-3680. (f) Légaré, M-A.; Pranckevicius, C.; Braunschweig, H. Metallomimetic Chemistry of Boron. *Chem. Rev*. **2019**, *119*, 8231-8261.

(2) (a) Bag, P.; Porzelt, A.; Altmann, P. J.; Inoue, S. A Stable Neutral Compound with an Aluminum–Aluminum Double Bond. *J. Am. Chem. Soc.* **2017**, *139*, 14384-14387. (b) Weetman, C.; Porzelt, A.; Bag, P.; Hanusch, F.; Inoue, S. Dialumenes – Aryl vs. Silyl Stabilisation for Small Molecule Activation and Catalysis. *Chem. Sci*. **2020**, *11*, 4817-4827.

(3) (a) Braunschweig, H.; Dellermann, T.; Dewhurst, R. D.; Ewing, W. C.; Hammond, K.; Jimenez-Halla, J. O. C.; Kramer, T.; Krummenacher, I.; Mies, J.; Phukan, A. K.; Vargas, A. Metal-Free Binding and Coupling of Carbon Monoxide at a Boron–Boron Triple Bond. *Nat. Chem*. **2013**, *5*, 1025-1028. (b) Böhnke, J.; Braunschweig, H.; Dellermann, T.; Ewing, W. C.; Hammond, K.; Jimenez-Halla, J. O. C.; Kramer, T.; Mies, J. The Synthesis of $B_2(SIDip)_2$ and its Reactivity Between the Diboracumulenic and Diborynic Extremes. *Angew. Chem., Int. Ed.* **2015**, *54*, 13801-13805. (c) Arrowsmith, M.; Böhnke, J.; Braunschweig, H.; Celik, M. A.; Dellermann, T.; Hammond, K. Uncatalyzed Hydrogenation of First-Row Main Group Multiple Bonds. *Chem. Eur. J*. **2016**, *22*, 17169-17172. (d) Arrowsmith, M.; Boehnke, J.; Braunschweig, H.; Celik, M. A.; Claes, C.; Ewing, W. C.; Krummenacher, I.; Lubitz, K.; Schneider, C. Neutral Diboron Analogues of Archetypal Aromatic Species by Spontaneous Cycloaddition. *Angew. Chem., Int. Ed*. **2016,** *55*, 11271-11275. (e) Stennett, T. E.; Bertermann, R.; Braunschweig, H. Construction of Linear and Branched Tetraboranes by 1,1- and 1,2-Diboration of Diborenes. *Angew. Chem., Int. Ed*. **2018,** *57*, 15896-15901. (f) Brückner, T.; Dewhurst, R. D.; Dellermann, T.; Müller, M.; Braunschweig, H. Mild Synthesis of Diboryldiborenes by Diboration of B–B Triple Bonds. *Chem. Sci.* **2019,** *10*, 7375-7378. (g) Brückner, T.; Stennett, T. E.; Heß, M.; Braunschweig, H. Single and Double Hydroboration of B–B Triple Bonds and Convergent Routes to a Cationic Tetraborane. *J. Am. Chem. Soc.* **2019,** *141*, 14898-14903. (h) Stennett, T. E.; Jayaraman, A.; Brückner, T.; Schneider, L.; Braunschweig, H. Hydrophosphination of Boron–Boron Multiple Bonds. *Chem. Sci.* **2020,** *11*, 1335-1341.

(4) (a) Power, P. P. Interaction of Multiple Bonded and Unsaturated Heavier Main Group Compounds with Hydrogen, Ammonia, Olefins, and Related Molecules. *Acc. Chem. Res.* **2011**, *44*, 627-637. (b) Hanusch, F.; Groll, L.; Inoue, S. Recent Advances of Group 14 Dimetallenes and Dimetallynes in Bond Activation and Catalysis. *Chem. Sci.* **2021**, DOI: 10.1039/d0sc03192e.

(5) Peng, Y.; Ellis, B. D.; Wang, X.; Fettinger, J. C.; Power, P. P. Reversible σ-Complexation of Ethylene by Main Group Molecules under Ambient Conditions. *Science* **2009**, *325*, 1668–1670.

(6) Wang, S.; Sherbow, T. J.; Berben, L. A.; Power, P. P. Reversible Coordination of H_2 by a Distannyne. *J. Am. Chem. Soc*. **2018**, *140*, 590-593.

(7) Sugahara, T.; Guo, J.-D.; Sasamori, T.; Nagase, S.; Tokitoh, N. Regioselective Cyclotrimerization of Terminal Alkynes Using a Digermyne. *Angew. Chem., Int. Ed.* **2018**, *57*, 3499-3503.

(8) Weetman, C.; Bag, P.; Szilvasi, T.; Jandl, C.; Inoue, S. CO_2 Fixation and Catalytic Reduction by a Neutral Aluminum Double Bond. *Angew. Chem., Int. Ed.* **2019**, *58*, 10961-10965.

(9) Ogawa, T.; Ruddy, A. J.; Sydora, O. L.; Stradiotto, M.; Turculet, L. Cobalt- and Iron-Catalyzed Isomerization–Hydroboration of Branched Alkenes: Terminal Hydroboration with Pinacolborane and 1,3,2-Diazaborolanes. *Organometallics* **2017**, *36*, 417-423.

(10) Arrowsmith, M.; Böhnke, J.; Braunschweig, H.; Deißenberger, A.; Dewhurst, R. D.; Ewing, W. C.; Hörl, C.; Mies, J.; Muessig, J. H. Simple Solution-Phase Syntheses of Tetrahalodiboranes(4) and Their Labile Dimethylsulfide Adducts. *Chem. Commun.* **2017**, 53, 8265-8267.

(11) Braunschweig, H.; Dewhurst, R. D.; Hammond, K.; Mies, J.; Radacki, K.; Vargas, A. Ambient-Temperature Isolation of a Compound with a Boron-Boron Triple Bond. *Science* **2012**, *336*, 1420-1422.

(12) Braunschweig, H.; Dewhurst, R. D.; Hoerl, C.; Phukan, A. K.; Pinzner, F.; Ullrich, S. Direct Hydroboration of B=B Bonds: A Mild Strategy for the Proliferation of B-B Bonds. *Angew. Chem., Int. Ed.* **2014**, *53*, 3241-3244.

(13) Bissinger, P.; Braunschweig, H.; Damme, A.; Kupfer, T.; Vargas, A. Base-Stabilized Diborenes: Selective Generation and η^2 Side-on Coordination to Silver(I). *Angew. Chem., Int. Ed.* **2012**, *51*, 9931.

(14) Bissinger, P.; Braunschweig, H.; Damme, A.; Hoerl, C.; Krummenacher, I.; Kupfer, T. Boron as a Powerful Reductant: Synthesis of a Stable Boron-Centered Radical-Anion Radical-Cation Pair. *Angew. Chem., Int. Ed.* **2015**, *54*, 359-362.

(15) Braunschweig, H.; Constantinidis, P.; Dellermann, T.; Ewing, W. C.; Fischer, I.; Hess, M.; Knight, F. R.; Rempel, A.; Schneider, C.; Ullrich, S.; Vargas, A.; Woollins, J. D. Highly Strained Heterocycles Constructed from Boron-Boron Multiple Bonds and Heavy Chalcogens. *Angew. Chem., Int. Ed.* **2016**, *55*, 5606-5609.

(16) Braunschweig, H.; Krummenacher, I.; Lichtenberg, C.; Mattock, J. D.; Schaefer, M.; Schmidt, U.; Schneider, C.; Steffenhagen, T.; Ullrich, S.; Vargas, A. Dibora[2]ferrocenophane: A Carbene-Stabilized Diborene in a Strained cis-Configuration. *Angew. Chem., Int. Ed.* **2017**, *56*, 889-892.

(17) Wang, S. R.; Arrowsmith, M.; Boehnke, J.; Braunschweig, H.; Dellermann, T.; Dewhurst, R. D.; Kelch, H.; Krummenacher, I.; Mattock, J. D.; Muessig, J. H.; Thiess, T.; Vargas, A.; Zhang, J. Engineering a Small HOMO-LUMO Gap and Intramolecular C-H Borylation by Diborene/Anthracene Orbital Intercalation. *Angew. Chem., Int. Ed.* **2017**, *56*, 8009-8013.

(18) Stennett, T. E.; Mattock, J. D.; Pentecost, L.; Vargas, A.; Braunschweig, H. Chelated Diborenes and Their Inverse-Electron-Demand Diels-Alder Reactions with Dienes. *Angew. Chem., Int. Ed.* **2018**, *57*, 15276-15281.

(19) Muessig, J. H.; Thaler, M.; Dewhurst, R. D.; Paprocki, V.; Seufert, J.; Mattock, J. D.; Vargas, A.; Braunschweig, H. Phosphine-Stabilized Diiododiborenes: Isolable Diborenes with Six Labile Bonds. *Angew. Chem., Int. Ed.* **2019,** *58*, 4405-4409.

(20) Stennett, T. E.; Bissinger, P.; Griesbeck, S.; Ullrich, S.; Krummenacher, I.; Auth, M.; Sperlich, A.; Stolte, M.; Radacki, K.; Yao, C.-J.; Wuerthner, F.; Steffen, A.; Marder, T. B.; Braunschweig, H. Near-Infrared Quadrupolar Chromophores Combining Three-Coordinate Boron-Based Superdonor and Superacceptor Units. *Angew. Chem., Int. Ed.* **2019**, *58*, 6449-6454.

(21) Bissinger, P.; Braunschweig, H.; Celik, M. A.; Claes, C.; Dewhurst, R. D.; Endres, S.; Kelch, H.; Kramer, T.; Krummenacher, I.; Schneider, C. Synthesis of Cyclic Diborenes with Unprecedented cis-Configuration. *Chem. Commun.* **2015**, *51*, 15917-15920.

(22) Arrowsmith, M.; Boehnke, J.; Braunschweig, H.; Celik, M. A.; Dellermann, T.; Hammond, K. Uncatalyzed Hydrogenation of First-Row Main Group Multiple Bonds. *Chem. - Eur. J.* **2016**, *22*, 17169-17172.

(23) Auerhammer, D.; Arrowsmith, M.; Bissinger, P.; Braunschweig, H.; Dellermann, T.; Kupfer, T.; Lenczyk, C.; Roy, D. K.; Schaefer, M.; Schneider, C. Increasing the Reactivity of Diborenes: Derivatization of NHC-Supported Dithienyldiborenes with Electron-Donor Groups. *Chem. - Eur. J.* **2018**, *24*, 266-273.

(24) Wang, Y.; Quillian, B.; Wei, P.; Wannere, C. S.; Xie, Y.; King, R. B.; Schaefer, H. F., III; Schleyer, P. v. R.; Robinson, G. H. A Stable, Neutral Diborene Containing a B=B Double Bond. *J. Am. Chem. Soc.* **2007,** *129*, 12412-12413.

(25) Lu, W.; Li, Y.; Ganguly, R.; Kinjo, R. Alkene–Carbene Isomerization Induced by Borane: Access to an Asymmetrical Diborene. *J. Am. Chem. Soc.* **2017,** *139*, 5047-5050.

(26) Stoy, A.; Boehnke, J.; Jimenez-Halla, J. O. C.; Dewhurst, R. D.; Thiess, T.; Braunschweig, H. CO_2 Binding and Splitting by Boron-Boron Multiple Bonds. *Angew. Chem., Int. Ed.* **2018,** *57*, 5947-5951.

(27) (a) Chong, C. C.; Kinjo, R. Catalytic Hydroboration of Carbonyl Derivatives, Imines, and Carbon Dioxide. *ACS Catalysis* **2015**, *5*, 3238-3259. (b) Hadlington, T. J.; Kefalidis, C. E.; Maron, L.; Jones, C. Efficient Reduction of Carbon Dioxide to Methanol Equivalents Catalyzed by Two-Coordinate Amido–Germanium(II) and −Tin(II) Hydride Complexes. *ACS Catalysis* **2017,** *7*, 1853-1859.

(28) Leong, B.-X.; Teo, Y.-C.; Condamines, C.; Yang, M.-C.; Su, M.-D.; So, C.-W. A NHC-Silyliumylidene Cation for Catalytic N-Formylation of Amines Using Carbon Dioxide. *ACS Catalysis* **2020**, *10*, 14824–14833.

(29) Blondiaux, E.; Pouessel, J.; Cantat, T. Carbon Dioxide Reduction to Methylamines under Metal-free Conditions. *Angew. Chem., Int. Ed.* **2014,** *53*, 12186-12190.

(30) Chen, W.-C.; Shen, J.-S.; Jurca, T.; Peng, C.-J.; Lin, Y.-H.; Wang, Y.-P.; Shih, W.-C.; Yap, G. P. A.; Ong, T.-G. Expanding the Ligand Framework Diversity of Carbodicarbenes and Direct Detection of Boron Activation in the Methylation of Amines with CO_2. *Angew. Chem., Int. Ed.* **2015,** *54*, 15207-15212.

(31) Leong, B.-X.; Lee, J.; Li, Y.; Yang, M.-C.; Siu, C.-K.; Su, M.-D.; So, C.-W. A Versatile NHC-Parent Silyliumylidene Cation for Catalytic Chemo- and Regioselective Hydroboration. *J. Am. Chem. Soc.* **2019**, *141*, 17629-17636.

SYNOPSIS TOC